Nuclear Instruments and Methods in Physics Research B 369 (2016) 60–65

Contents lists available at ScienceDirect

Nuclear Instruments and Methods in Physics Research B

journal homepage: www.elsevier.com/locate/nimb

Photoemission spectroscopy of planar and nanostructured surfaces

J.L. Gervasoni

Centro Atomico Bariloche and Instituto Balseiro (CNEA), 8400 Bariloche, Rio Negro, Argentina

ARTICLE INFO

Article history:
Received 6 July 2015
Received in revised form 28 September 2015
Accepted 29 September 2015
Available online 22 October 2015

Keywords:
Photoemission spectroscopy surfaces

ABSTRACT

In this paper, I present some results for the process of excitation of bulk and surface plasmons during the emission of electrons in the proximity of surfaces of different shapes and dimensions. I describe in detail the effects due to the interaction between an electron and a stationary positive ion (or atomic hole) in the neighborhood of a metallic surface, paying special attention to the results obtained by my research group. We used the dielectric response of the metal and the specular reflection model for the case of planar surfaces, and the second quantization theory for nanostructured surfaces. In particular, we studied how the electron–hole pair interaction can influence the energy loss of the emerging electron. We investigated the importance of surface effects in the analysis of photoelectron spectroscopy. The method described here is useful for studying multiple plasmon excitations in nanostructures and for understanding the excited electron spectra of these nanostructures (different from those of the same bulk material).

1. Introduction

The properties of solid surfaces or interfaces, in particular with respect to interactions with gases and fluids, are topics of current technological interest. They play an important role in processes such as heterogeneous catalysis, physics of semiconductors and thin films, or protection against corrosion. These applications have led to the development of various tools for studying surfaces. In particular, the use of various spectroscopy and surface analysis techniques have had a major impact on the development of this area. The usual techniques for the study of surfaces make use of particles such as photons, electrons, atoms, molecules and ions as analysis tools. Which one is used depends on the required information, referring either to the surface crystallographic structure, composition, chemical bonds or surface vibrations. It also depends on how selective one must be in the number of surface atomic layers investigated. The natural way to fulfil this requirement is by adjusting the mass and energy of the particles. Among the available particles, electrons have found the widest application for several reasons. For instance, they have a mean free path of tens of Å, depending of their energy, which makes them appropriate to analyze excitations characteristics of the surface region of a solid. In addition, they offer efficient techniques for production, detection and analysis (in angle and energy) of electron beams [1].

The different types of electron spectroscopy can be divided into two subgroups. In the first, the surface is bombarded with an electron beam. Then, the electrons scattered by the surface, or the secondary electrons emitted in the process, are analyzed in angle or energy. Within this subgroup, low energy electron diffraction technique (LEED) has been one of the most widely used for the investigation of the surface structure. The most important impediment of this surface crystallography technique lies in the considerable theoretical difficulty involved in the analysis of the intensities. Another technique in this subgroup is Auger electron spectroscopy (AES). Here the primary electron generates a vacancy in an internal atomic level, which is later occupied by a valence electron. The energy resulting from this transition is delivered to a second electron, which escapes from the material and is analyzed. This AES technique is preferably used to analyze elements or their traces, existing in a sample. In the second group of electron spectroscopy, they are generated through irradiation of the material with photons originated in an external source. Spectroscopy of electrons excited by photons has attracted much attention, stimulated by the availability of continuous synchrotron radiation sources. However most of the experiments are performed with conventional continuous sources. These techniques are often distinguished between Ultraviolet Photoemission Spectroscopy (UPS), for variable energies between 10 and 1000 eV, and induced X-ray Photoemission Spectroscopy (XPS), for fixed energies in the range of keV. Typically, Al K_α and Mg K_α lines are used, with energies of 1486.6 eV and 1253.6 eV respectively.

Although these techniques of electron spectroscopy on surfaces have been used successfully, and that the vast majority of our knowledge about surfaces comes from one or other electron spectroscopy, it should be noted that the use of electrons as carriers of

E-mail address: gervason@cab.cnea.gov.ar

http://dx.doi.org/10.1016/j.nimb.2015.09.088
0168-583X/

information about surface has certain inherent limitations. In general, these techniques require very good vacuum conditions ($<10^{-10}$ torr) for normal operation. Unfortunately, these requirements make spectroscopy of surfaces in real situations technically impossible. Even such analysis of *in situ* surfaces, after evacuating the gas, is of limited value, since such action can change the conditions of the surface. Thus the use of ultra-high vacuums, which is generally considered as an advantage since it allows studying the stable surfaces under controlled conditions, represents an inconvenience for many situations of technical interest, especially in relation to the study of catalysis and corrosion. The need of analytical techniques, which would operate even when the surface is in contact with liquids or gases at high pressure, remains one of the greatest challenges of Surface Physics. The techniques of Scanning Tunneling Microscopy (STM) [2] and Atomic Force Microscopy (AFM) [3] are partially helping to solve this difficult problem [4].

Another limitation comes from the fact that electron spectroscopies are destructive in general, especially when techniques requiring high currents are used. The energy provided by the primary or secondary electrons may be sufficient to produce chemical reactions. For example the cross sections for desorption of gases by electronic stimulation can reach values of about 10^{-15} cm^2 [5]. That is how incident beams of a few nanometers in diameter, as used for example in Auger spectroscopy, can cause the stimulated desorption of stable adsorbed elements. This makes these techniques not suitable for analysis of adsorbed surface layers. Only for the atoms of the substrate, the stimulated desorption can be neglected.

As discussed below, even another limitation comes from the definition of the surface itself, i.e. the area to be analyzed by these techniques. As we said above, this largely depends on the energy of the electrons and on the characteristic of the material. In fact, these techniques do not analyze the surface properties in a strict sense, but the properties of the medium, with a penetration depth that can be adjusted by varying the conditions of the experiment.

In spite of these limitations, the AES and XPS techniques [6] have proved to be very useful tools for nanostructure characterization [7–10], providing information on the composition and oxidation state of components [10]. Otherwise, many novel nanodevices have been developed recently, making the study of nanostructures of different (not only planar) geometrical shape important and necessary. The plasmon generation requires a special attention for nanocylinders and nanotubes, which are of interest in nanolasers [11], plasmonic circuitry [12] and aluminum nanorods in batteries [13]. These new developments require more accurate information on the process of plasmon generation.

In principle, the formalism developed in this work can be applied to various methods of electron emission spectroscopy (ie, AES, UPS and XPS). The application to the case of XPS that I discuss in this work is motivated by the greater availability of experimental data from various authors and for various elements; making it possible to establish a more comprehensive comparison with the results of the proposed theoretical model.

From the theoretical point of view, the interaction of an electron emitted by a nearby ion at the surface is also of current interest to understand the effects of dynamic electron–ion-surface interaction in the energy spectrum of the secondary electrons emitted in experiments of ion-surface [14,15] and ion–solid [16,17] interactions.

A widespread assumption in studies of secondary emission is the so-called three-step model: production of the electron, transport within the solid, and escape through the surface. The analysis of the obtained electron spectra usually uses this model [18] and the separation of the plasmon production into *extrinsic* and *intrinsic* contributions [19–22]. However these criteria are not always accurate, as in the case when the electron–hole pair is created near the surface, or for nanosized systems [23].

The purpose of this work is to fully investigate the interactions between an electron and a stationary ionic (or atomic) hole in the vicinity of a solid surface. In particular, I discuss how the energy dissipation and the corresponding probability of excite surface and bulk plasmons due to the emerging electron may be influenced by the sudden creation of a positive charge in planar and nano-sized surfaces. The theoretical tools are presented in the next section. In Section 3 I present the calculations and results, and in Section 4 I provide some concluding remarks.

2. Theoretical description

The emission of an electron in the proximity of a surface forms the basis of different techniques for surface analysis. One of the most popular is the X-ray induced Photoemission Spectroscopy (XPS) [6]. In such experiments, the emission of electrons from the internal shells of the atoms of the material is induced by irradiating it with photons of a typical X-ray source in the range of keV. The electron emission can also be induced by ion impact [24]. After the emission of the electron, it leaves a residual hole in the material, whose half-life of neutralization is greater than the characteristic time of flight of the emitted electron. As we will see in this paper, the sudden appearance of this hole strongly influences the probability of excitation of plasmon. The role of the hole created during emission is one of the most interesting problems that arise from this analysis.

2.1. Planar surfaces

We use the so-called specular reflection model [25,26] to describe the system and the involved fields, where the metal and the vacuum are treated as if they were infinite with symmetrized charge densities (see Fig. 1). The hole–electron pair is created at a distance z_o from the interface between the metal and the vacuum. We assume that the hole is fixed at $\mathbf{r}_o = (0, z_0)$ and that the emitted electron follows a uniform trajectory $\mathbf{r}_e = \mathbf{r}_o + \mathbf{u}t$, (being $\mathbf{u}$

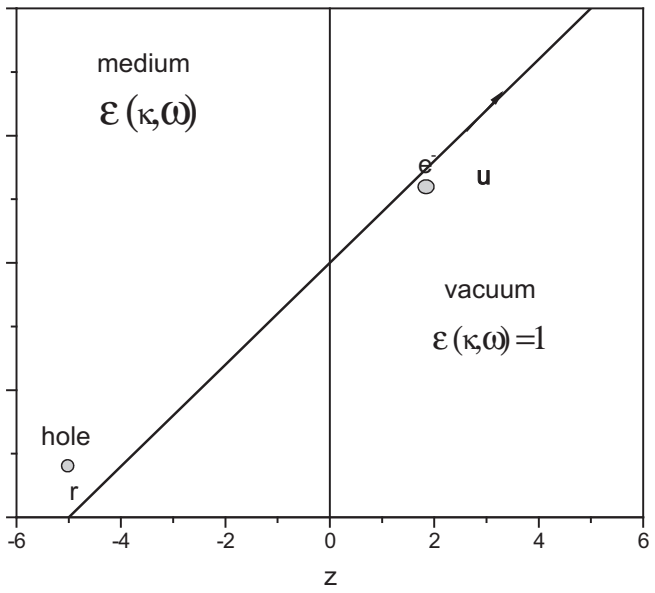

Fig. 1. Scheme of the process for planar surfaces: one electron is removed from the inner shell of the atom, leaving behind a hole in the material. In such a process, both the sudden creation of the pair and the escaping electron are responsible of plasmon generation in the medium.

the electron velocity, and t its time coordinate) perpendicular to the surface, which remains undisturbed by the plasmon excitation events. This approximation holds for enough large kinetic energies, $mu^2/2 \gg \hbar\omega_p$ [27], where ω_p is the characteristic plasmon frequency of the material. In X-ray photoemission spectroscopy (XPS) the emitted electron energy is in the keV range, and this approximation within our formalism is fully justified.

The charge densities incorporate the image charge of the hole (h'), the image charge of the electron (e') and a surface charge distribution (σ_M or σ_V, depending if the particles are in the extended medium or vacuum, respectively), which is necessary to match the boundary conditions. In this frame, the behavior of the material is determined by the local dielectric function [28]:

$$\varepsilon(k,\omega) = \varepsilon(\omega) = 1 - \omega_p^2/\omega(\omega + i\gamma), \tag{2.1.1}$$

with the corresponding values for the plasma frequency ω_p and the damping constant γ.

Throughout the paper, I use atomic units (au).

Following the same formalism developed in [25], the total energy dissipation rate due to the fields acting on the emitted electron is given by the induced potentials ϕ^{ind} in the medium, and the vacuum (with the adequate matching conditions),

$$\dot{W}_{dis}^{(q)} = (Z_j)\frac{\partial\phi^{ind}(r,t)}{\partial t}\Big|_{r=r(t)} = -i(Z_j)\int\frac{d^3k}{(2\pi)^3}\int\frac{d\omega}{(2\pi)}\omega\phi^{ind}(k,\omega)e^{i(k.r-\omega t)}\Big|_{r=r(t)} \tag{2.1.2}$$

where Z_j is the charge of the external particle (hole or electron), a parameter that takes different values depending on which process we are studying. For the case of the electron, Z_j is always equal to one, but, in the case of the hole, $Z_j = 1$ for the photoionization and $Z_j = 2$ for an Auger process.

Integrating in time the previous equation for the energy loss, we obtain the total energies absorbed by both (bulk and surface) plasmon fields. As the plasmons can also be excited due to the sudden creation of the core hole, these contributions must be added to the total energy. Finally, the average numbers of bulk (b) and surface (s) plasmons excited in an electron emission process occurring at a distance z from the surface of the solid material are:

$$Q^{\upsilon} = \frac{-1}{\hbar\omega_{\upsilon}}\left(\int \dot{W}_{dis}^{\upsilon}dt\right), \tag{2.1.3}$$

being υ = bulk (b) or surface (s) plasmons. We obtain

$$Q^b(z) = \frac{e^2}{2\hbar u}\Theta(-z) * \{f_{12}(0) - f_{12}(2\omega_p|z|/u) + 2\omega_p|z|/u)f_{11}(0) - 4f_{22}(0) + 4\exp(-\gamma|z|/u/2)*[\sin(\omega_p|z|/u)f_{23}(\omega_p|z|/u) + \cos(\omega_p|z|/u)f_{22}(\omega_p|z|/u)]\} \tag{2.1.3.a}$$

$$Q^s = \frac{e^2}{2\hbar u}\{2f_{00}(2\omega_s|z|/u) - f_{10}(2\omega_s|z|/u) - 4\Theta(-z)[f_{22}(0) - \exp(-\gamma|z|/2u)[\sin(\omega_s|z|/u)f_{23}(\omega_s|z|/u)] + \cos(\omega_s|z|/u)f_{22}(\omega_s|z|/u)]\} \tag{2.1.3.b}$$

where $\Theta(z)$ is the Heaviside function. The auxiliary functions $f_{mn}(t)$, valid for perpendicular trajectory, are defined as:

$$f_{nm}(t) = \int_0^{\xi} dx\frac{x^m}{(1+x^2)^n}\exp(-xt), \tag{2.1.4}$$

with $\xi = uk_c/\omega_l$, where ω_l is equal to ω_p for bulk plasmons and to $\omega_s = \omega_p/\sqrt{2}$ for surface plasmons, and k_c is the usual cut-off in the plasma dielectric response. The previous expressions are valid for both internal ($z < 0$) and external emission ($z > 0$). Note that, as expected from the specular reflection model, the terms related to the bulk plasmon excitations are zero for external emission, or after the electron escaped to the vacuum in the case of internal emission.

2.2. Nanostructures surfaces

For nanogeometries, the previous semi classical model is not applicable. As a working example, let us consider the interaction of the electron and the hole with the plasmon field [29] of a nano-cylinder (see scheme in Fig. 2) in the frame of the second quantization theory. Taking into account these interactions, the total Hamiltonian for the system is

$$H = H_0^{(s)} + H_0^{(b)} + H_{\text{int}}(t) \tag{2.2.1}$$

where $H_0^{(s)}$ and $H_0^{(b)}$ are the Hamiltonians for the surface and the bulk, respectively. We note that, since this process occurs inside the cylinder, both types of plasmons are generated. In the case of nanostructures, due to the high surface/volume ratio, mainly surface plasmons are generated. On the other side, $H_{\text{int}}(t)$ is the *interaction term*, which refers to the interaction of the electron gas of the medium with the electron and the hole. Here we shall not consider any direct interaction between the hole and the electron. Thus we write, $H_{\text{int}}(t) = -e\phi_s^e\Theta(t-t_0) + e\phi_s^h\Theta(t-t_0)\Theta(T_h - t)$, where ϕ_s^e is the electrostatic potential due to the electron, ϕ_s^h is the electrostatic potential due to the hole, Θ is the *Heaviside* function, t_0 is the time when the electron–hole pair is created, and T_h is the time when the hole vanishes. In the frame of the *coherent states* formulation [30], the wave function, i.e. the solution of the time-dependent Schrödinger equation [30], has the form:

$$|\Psi(t)\rangle = \exp\left[-i\sum_{m,k}X_m^{(s)}(k,t)a_{m,k} + X_m^{(s)*}(k,t)a_{m,k}^{\dagger}\right]. \tag{2.2.2}$$

The function $X_m^{(s)}(k)$ is given by

$$X_m^{(s)}(k) = -\frac{Ze}{\hbar}\int_0^T f_m(k,t)e^{-i\omega_m t}dt + \frac{Ze}{\hbar}\int_0^{T_h} f_m^{(h)}(k,t)e^{-i\omega_m t}dt \tag{2.2.3}$$

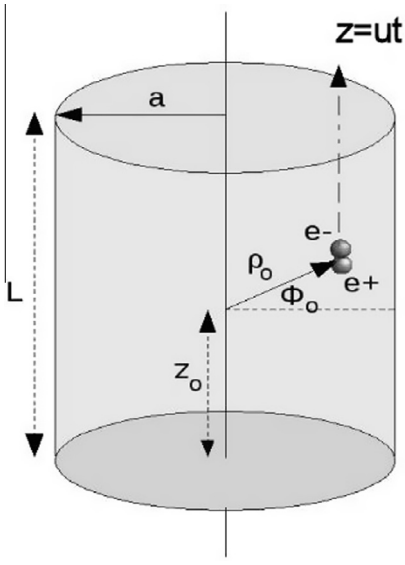

Fig. 2. Scheme of the process for nano-surfaces An electron–hole pair was created at time $t = 0$, and the electron escapes from a nanocylinder in a given trajectory, while the hole remains stationary at a radial distance ρ_0 from the cylinder axis.

with

$$f_m(k,t) = \lambda_m(k) I_m(k\rho) e^{i(kz(t)+m\phi)} \text{ and } f_m^{(h)}(k,t) = \lambda_m(k) I_m(k\rho_h) e^{i(kz_h(t)+m\phi_h)} \quad (2.2.4)$$

The limit T in the integral (2.2.3) is the time when the electron reaches the surface. The parameter $\lambda_m(k)$ is defined as: $\lambda_m(k) = \sqrt{\frac{\omega_m K_m(ka)}{I I_m(ka)}}$; and ω_m, for $m = 0, 1, 2, \ldots$, represent the allowed oscillation frequency modes for the charge density of the electron gas, and is obtained by the appropriate dispersion relation for cylinders [31]. Finally, T_h corresponds to the time elapsed until the hole decays.

The previous equations are valid for any trajectory of the electron *inside* the material.

Finally, the rate of the surface plasmon production due to the influence of the electron and the hole in the system, in the m mode is (as a function of momentum k) [32]:

$$Q_m(k) = \frac{L}{2\pi} |X_m^{(s)}(k)|^2 \quad (2.2.5)$$

where L is the length of the cylinder. Then, the average number of produced plasmons is:

$$Q_m = \int_0^\infty Q_m(k) dk. \quad (2.2.6)$$

This leads to a three-term expression for the plasmon production, whatever the trajectory of the electron is: $Q_m = Q_m^{(e)} + Q_m^{(h)} + Q_m^{(eh)}$, where the electron contribution is denoted by $Q_m^{(e)}$, the hole contribution by $Q_m^{(h)}$, and the electron–hole term by $Q_m^{(eh)}$ (sometimes called *interference term*).

3. Results

3.1. Planar surfaces

Let us begin by analyzing whether the previous Eq. (2.1.3) can be separated in:

$$Q^b = \frac{-1}{\hbar\omega_p} \left(\int \dot{W}_{ext}^b dt + \int \dot{W}_{int}^b dt \right) \quad (3.1.1.a)$$

$$Q^s = \frac{-1}{\hbar\omega_s} \left(\int \dot{W}_{ext}^s dt + \int \dot{W}_{int}^s dt \right). \quad (3.1.1.b)$$

where the different contributions (extrinsic "ext", intrinsic "int") for the energy loss correspond to the commonly accepted definition [25]. Moreover, since not all the detected electrons come from the same depth, it is necessary to average (integrate) these distributions in these different depths (coordinate z). Let us note that, when Eq. (2.1.3) are employed, this integral cannot be solved in closed form.

Neglecting begrenzung effects, and using for the integral the asymptotic values of Q (suggested by Mahan [24]), we obtain for Q^b and Q^s the so called extrinsic and intrinsic contributions:

$$Q_{ext}^b(z) \cong \frac{e^2\omega_p}{\hbar u^2} \theta(-z) * |z| f_{11}(0) \quad (3.1.1.a1)$$

$$Q_{int}^b(z) \cong \frac{e^2}{2\hbar u} \theta(-z) * \{f_{12}(0) - 4f_{22}(0)\} \quad (3.1.1.a2)$$

$$Q_{ext}^s \cong \frac{e^2}{2\hbar u} \{2f_{00}(2\omega_s|z|/u) - f_{10}(2\omega_s|z|/u)\} \quad (3.1.1.b1)$$

$$Q_{int}^s \cong \frac{e^2}{\hbar u} 2\{\theta(-z) f_{22}(0)\} \quad (3.1.1.b2)$$

These expressions coincide with those obtained by other authors [20], and are frequently used in the analysis of experimental results [18].

In order to compare both contributions (extrinsic and intrinsic) and both XPS and AES processes, we consider only internal emission ($z < 0$). We apply our results to aluminum (metal) and to silicon (semiconductor). In Figs. 3 and 4 we plotted the average number of bulk and surface plasmons, respectively, as a function of t_o, i.e. the instantaneous time when the electron, is emitted in XPS processes. We consider the emission of an electron with velocity $u = 4$ au as a function of the distance z_o between the hole and the surface inside aluminum ($\omega_p = 0.56$ and $\gamma = 0.035$ [25]) and silicon ($\omega_p = 0.62$ and $\gamma = 0.156$ [25]). We separate the terms related to the so-called extrinsic and intrinsic contributions in order to obtain the difference in the average number of bulk ($i = B$) or surface ($i = S$) plasmons excited in both processes. An important point to take into account is that these quantities, in order to have a clear physical sense, must be positive: they are an average number of excited plasmons.

For surface plasmons we observe that, separating the contributions to the total average number of plasmons in extrinsic and intrinsic as independent processes, for the case when the distance between the place of the creation of the electron–hole and the surface is small, the extrinsic contribution gives an unphysical value (negative values), which gives an idea about whether there can be some interference process going on.

The behavior for bulk plasmons follows the same characteristic than those for surface plasmons, but now the division between extrinsic and intrinsic seems plausible, due to the fact that the production of bulk plasmons goes quickly to zero in the proximity of the surface, when the interference processes are more important (in contrast, surface plasmons have a high peak near the surface).

3.2. Nanostructures surfaces

We now use our model to study an aluminum ($\omega_P = 0.58$) cylindrically-shaped nanorod of typical nanoscale dimensions: radius $a = 20.0$ au. ($\approx$1 nm), and length $L = 200$ au. ($\approx$10 nm). Aluminum nanorods are very important in nanomaterials applications [12] and they are also relatively easy to produce [13].

3.2.1. Parallel trajectory

Since we consider only the process until the moment when the electron reaches the surface, we assume that the time when the hole vanishes $T_h = T$ is the limit of integration in Eq. (2.2), to get:

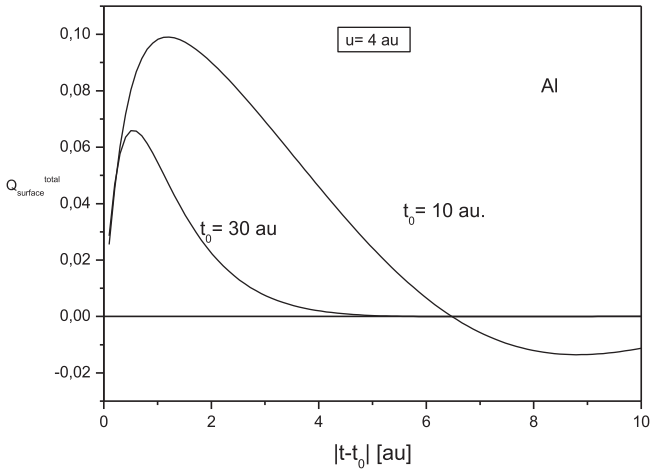

Fig. 3. Average number of bulk plasmons in aluminum, as a function of t_o, the instantaneous time of the emitted electron, for photoemission process (XPS).

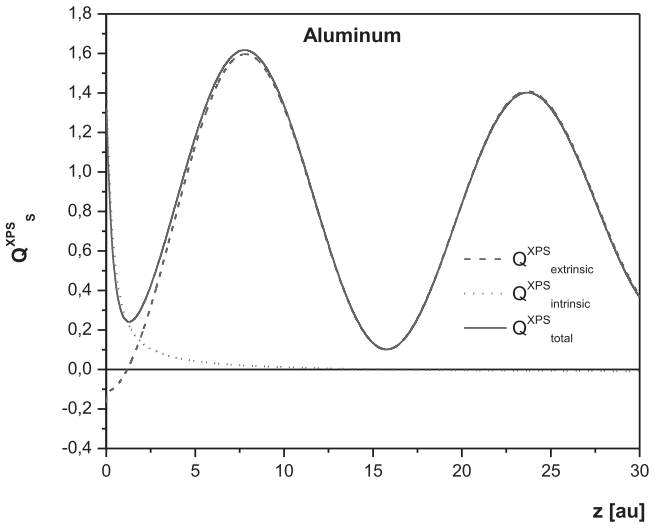

Fig. 4. Average number of surface plasmons in aluminum, as a function of t_o, the instantaneous time of the emitted electron, for photoemission process (XPS).

$$|X_m^{(s)}(k)|^2 = \lambda_m^2(k) I_m^2(k\rho)\Big\{(2/(k\nu-\omega_m))^2 sin^2[(k\nu-\omega_m)T/2] + (2/(-\omega_m))^2 sin^2[-\omega_m T/2] + sin((k\nu-\omega_m)T/2) \times sin[-\omega_m T/2] cos[k\nu T/2](8/((k\nu-\omega_m)\omega_m))\} \quad (3.2.1)$$

The time T when the electron reaches the nano surface is $T = (L - z_0)/v$; the factor $\lambda_m(k)$ is defined in Section 2.1, and ω_m are the available oscillation frequency modes for the charge density of the electron gas, and are obtained by the appropriate dispersion relation for cylinders.

In Fig. 5 we plotted $Q_m(k)$ as a function of the momentum k of the emerging electron. The electron–hole pair is suddenly generated at a distance $\rho_0 = 10$ au from the cylinder axis, and the electron escapes with velocity of 4 au. We see the different contributions of m to the total plasmon excitation. These contributions increase when the electron–hole creation coordinate approaches the surface, and has a minimum at the axis of the cylinder. In this latter case, unlike the modes $m \geqslant 1$, the mode $m = 0$ doesn't vanish there. The contribution from the hole behaves in a similar way, but the values of the curve are approximately one order of magnitude lower. This means that the electron contribution in this kind of process is dominating. As it can be seen from the equations and the figure, the electron contribution is strongly dominating over the hole contribution, in surface plasmon production. This phenomenon was observed previously [34] and can be attributed to the fact that once the electron is released, it interacts with the electron gas inside the cylinder for a long time.

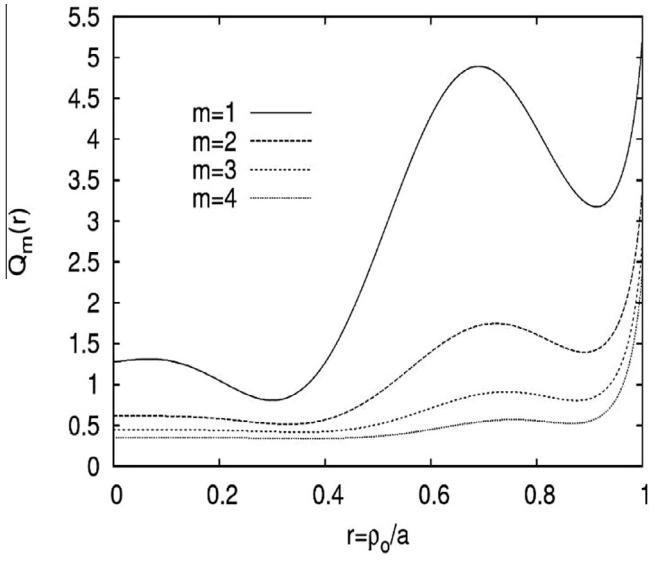

Fig. 5. Contribution of the principal m-modes to the plasmon generation per unit length, for a cylinder of radius $a = 20$ au as a function of the relative hole-to-axis distance $r = \rho_0/a$ for a given velocity of the electron $v = 4$ au, and trajectory parallel to the axis of the tube.

3.2.2. Radial trajectory

The cylinder is the same as in the parallel case but here the electron–hole pair is created at a radial distance ρ_0, then the electron leaves the hole and follows a radial trajectory $z(t) = z = \text{const.}$, $\phi = \text{const.}$, $\rho(t) = ut + \rho_0$. Replacing in Eqs. (2.2.3), (2.2.4), (2.2.5), we obtain,

$$|X_m^{(s)}(k)| = \lambda_{k,m}^2\Big\{(\Re e[Z_m(k)])^2 + (\Im m[Z_m(k)])^2 + [I_m(k\rho_0)]^2 sin^2(-\omega_m T_h/2)(2/\omega_m)^2 - (4/\omega_m) I_m(k\rho_0)\Re e[Z_m(k)] sin(-\omega_m T_h/2) cos(\omega_m T_h/2)\} \quad (3.2.2)$$

With:

$$\Re e[Z_m(k)] = \int_0^T I_m[k(vt+\rho_0)] cos(\omega_m t) dt \text{ and } \Im m[Z_m(k)] = \int_0^T I_m[k(vt+\rho_0)] sin(\omega_m t) dt \quad (3.2.3)$$

As in the parallel case, the first two terms in Eq. (3.2.2) represent the pure electron contribution, the third term corresponds to the pure contribution from the hole, and the fourth is the interference term.

In Fig. 6 we plot the electron contribution to Q_m as a function of $r = \rho_0/a$. This behavior is explained, in part, by the fact that (1) the electron must travel a path across the material before leaving the cylinder. During its travel inside the material, the time for the electron to interact with the medium becomes the longer, the deeper the electron–hole pair creation occurs, and thus the number of excited plasmons becomes higher; (2) the electron-surface interaction becomes stronger close to the surface intersected by the trajectory of the electron. The last term, according to Eq. (2.2.6), using (3.2.2), is sometimes called *interference* term and is negative since its effect reduces the total energy loss, as it was shown previously by other authors for aluminum nanosystems

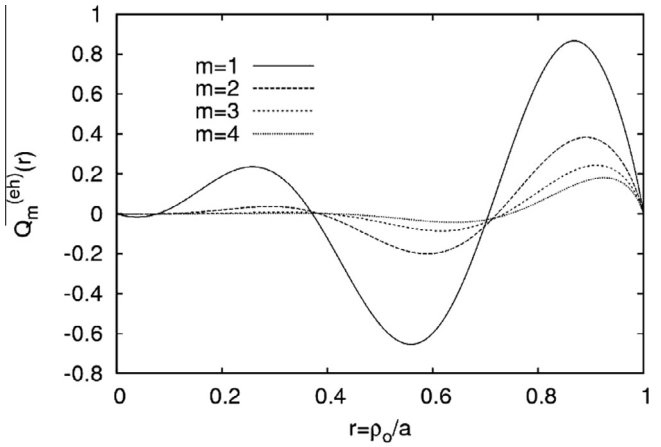

Fig. 6. Contribution of the principal m-modes to the plasmon generation per unit length, for a cylinder of radius $a = 20$ au as a function of the relative hole-to-axis distance $r = \rho_0/a$ for a given velocity of the electron $v = 4$ au., and radial trajectory.

[35]. The contribution of the hole increases continuously towards the surface and reflects the fact that the intrinsic contribution depends strongly on the surface [36]. As we can see from this figure, due to its magnitude, the interference term is not negligible, and the total plasmon production cannot be divided into just two terms named "intrinsic" and "extrinsic".

4. Concluding remarks

In summary, for planar surfaces, we have used the dielectric function formalism and the specular reflection model, together with the pseudo-extended medium, for studying the excitation of plasmons during the emission of electrons in the proximity of a solid surface. We investigated in detail the different contributions to the processes of photoemission (valid also for Auger electron emission). We showed that in the presence of surfaces, there are important differences with respect to the case of infinite mediums (or when the creation of the electron–hole pair is far from the surface), in the sense that there are important interference processes among the different contributions when the creation is near the surface, giving rise to "begrenzung" effects [25].We observed that the approximate model overestimates the probability of exciting surface plasmons and fails to give the probability of exciting bulk plasmon at moderate velocities. In this case we cannot separate the extrinsic and intrinsic contributions, neither in the so-called three-step model, nor in terms of independent processes.

Our results for the integrated energy loss and probabilities of excitations agree with existing results published earlier, if a simple plasmon-pole dielectric function is assumed, as it is the case for the materials studied in this work. In fact, both materials could be treated by using the same approximation, i.e. aluminum, because it is a typical metal, and silicon, which is a typical semiconductor. For the case of the excitation of plasmons, the single-pole approximation can also be used, although with a finite damping [28]. Moreover, we note that our general formulation of the problem through the dielectric approach also enables the study of the effects arising from different response functions (different materials).

About the analysis in nano-scaled systems: in particular, we studied the plasmon generation by an electron–hole pair in the case of cylindrical rods of aluminum. As we see, in the case of a *parallel trajectory* (i.e. parallel to the axis of the cylinder), the electron contribution to plasmon production is predominating, and the process can be considered as mainly *extrinsic*. According to this, neither the presence of the hole nor the sudden creation of the pair are dominant process for plasmon production in this configuration.

However, in the *radial trajectory* case, we note that due to the fact that the electron–hole term is large compared to the pure hole term, we can no longer consider the total plasmon production as the sum of only two terms, describing the contributions from the intrinsic and extrinsic excitations [36]. We conclude from this, that the trajectory of an emerging electron is a critical issue in order to determine if the separation in *extrinsic* or *intrinsic* terms is possible, and a very careful analysis must be done in order to compare plasmon spectra. In the case when the electron–hole term is large compared to the pure hole term, we can no longer consider the total plasmon excitation as the simple sum of the contributions of the electron and the hole; instead, we have to take into account the *interference* process that takes place during the interaction. We note that, due to this important interference process, the assumption on the separability between extrinsic and intrinsic terms must be revised. The application of this formalism to cases of experimental interest in XPS and AES is currently under way.

Acknowledgements

I want to acknowledge the collaboration of the following researchers: L. Kover, N. Arista, S. Segui, R. Barrachina, Z. Miskovic, W. Werner, and J. Garcia Gallardo.

This work was partially supported by the Research and Innovation Foundation (Hungary) and Secyt (Argentina) in the frame of the intergovernmental cooperation in science and technology between Hungary and Argentina (SCyT-NKTH), proyecto ARG-HA as well as by the projects: OTKA T038016 (Hungary) and Project PICT R2002-00,122 from the Ministerio de Ciencia, Tecnologia e Innovacion Productiva (MINCyT, Argentina).

References

[1] H. Ibach, Electron Spectroscopy for Surface Analysis, Springer-Verlag, Berlin, 1977.
[2] G. Binning, H. Roher, Rev. Mod. Phys. 59 (1987) 615.
[3] G. Binning, C.F. Qaute, Ch. Gerber, Phys. Rev. Lett. 56 (1986) 930.
[4] J.S. Murday, R.J. Colton, Proximal probes, techniques for measuring at the nanometer scale, in: R. Vanselow, R. Howe (Eds.), Chemistry and Physics of Solid Surfaces VIII, Springer-Verlag, Berlin, 1990.
[5] T.E. Madey, J.T. Yates, J. Vac. Sci. Technol. 8 (1971) 525.
[6] D.P. Woodruff, T.A. Delchar, Modern Techniques of Surface Science, Cambridge Univ. Press, UK, 1994.
[7] Y. Sohn, K.T. Leung, A. Radi, D. Pradhan, ACS Nano 4 (2010) 1553.
[8] M.G. Silly, F. Sirotti, P. Reiss, O. Renault, K. Haung, R. Demadrille, ACS Nano 4 (2010) 4799.
[9] M. Cheng, C. Hemminger, R. Penner, F. Yang, S. Kung, ACS Nano 4 (2010) 5233.
[10] M. Levendorf, W. Sang-Yong Ju, J. Edgeworth, X. Li, C.W. Magnuson, A. Velamakanni, R. Piner, J.K. Park, S. Chen, L. Brown, R.S. Ruoff, ACS Nano 5 (2011) 1321.
[11] J. Johnson, H. Choi, Nat. Mater. 1 (2002) 106.
[12] A.L. Falk, F.H.L. Koppens, C.L. Yu, K. Kang, N.D. Snapp, A.V. Akimov, M.H. Jo, M. D. Lukin, H. Park, Nat. Phys. 5 (2009) 475.
[13] Ch. Li, W. Ji, J. Chen, Z. Tao, Chem. Mater. 19 (2007) 5812.
[14] H. Winter, P. Strohmeier, J. Burgdorfer, Phys. Rev. A 39 (1989) 3895.
[15] H. Luth, Surfaces and Interfaces of Solid Materials, Springer-Verlag, Berlin, 1995.
[16] R. Raether, Excitations of plasmons and interband transitions by electrons, Springer Tracts in Modern Physics, vol. 88, Springer, Berlin, 1980.
[17] K.D. Sevier, Low Energy Electron Spectrometry, Wiley-Interscience, New York, 1972.
[18] W.S.M. Werner, Phys. Rev. B 52 (1995) 2964.
[19] F. Yubero, J.M. Sanz, B. Ramskov, S. Tougaard, Phys. Rev. B 53 (1996) 9719.
[20] F. Yubero, S. Tougaard, Phys. Rev. B 71 (2005) 045414.
[21] J.L. Gervasoni, F. Yubero, Nucl. Instrum. Methods B 182 (2001) 96–101.
[22] J.L. Gervasoni, L. Kövér, Surf. Interf. Anal. 38 (2006) 652.
[23] J.A. García Gallardo, J.L. Gervasoni, L. Kövér, Vacuum 84 (2010) 258.
[24] G.D. Mahan, Electron Spectroscopy of Solids, in: Dekeyser, Venik, Fiermans (Eds.), Plenum Press, New York, 1974.
[25] J.L. Gervasoni, N.R. Arista, Surf. Sci. 260 (1992) 329.
[26] C.D. Denton, J.L. Gervasoni, R.O. Barrachina, N.R. Arista, Phys. Rev. A 57 (1998) 4498.
[27] J.L. Gervasoni, L. Kover, Surf. Interface Anal. 38 (2006) 652–656.
[28] J. Lindhard, M. Scharff, Phys. Rev. 1 (24) (1961) 128.
[29] J.L. Gervasoni, N.R. Arista, Phys. Rev B 68 (2003) 235302.
[30] E. Merzbacher, Quantum Mechanics, 3rd ed., John Wiley & Sons, 1998.
[31] J.L. Gervasoni, L. Kövér, J. Electron Spectrosc. 161 (2007) 134.
[32] J.L. Gervasoni, L. Kövér, Vacuum 83 (2009) 1049.
[34] J.A. García Gallardo, J.L. Gervasoni, L. Kövér, Vacuum 84 (2010) 258.
[35] J.A. García Gallardo, J.L. Gervasoni, L. Kövér, J. Nanosci. Nanotechnol. 12 (2012) 9271.
[36] J.A. García Gallardo, J.L. Gervasoni, L. Kövér, Vacuum 107 (2014) 316.

Further reading

[33] N. Pauly, S. Tougaard, F. Yubero, Surf. Sci. 620 (2014) 17–22.